Theoretical Study of the Reaction Mechanism of BO, B_2O_2, and BS with H_2

Chih-Hao Chin,[†] Alexander M. Mebel,*[,‡,§] and Der-Yan Hwang*[,†]

Department of Chemistry, Tamkang University, Tamsui 25137, Taiwan, Institute of Atomic and Molecular Sciences, Academia Sinica, P.O. Box 23-166, Taipei 10764, Taiwan, and Department of Chemistry and Biochemistry, Florida International University, Miami, Florida 33199

Received: June 20, 2003; In Final Form: November 5, 2003

Potential energy surfaces of various reactions in the BO/H_2, B_2O_2/H_2, and BS/H_2 systems have been studied at the G2M(MP2)//B3LYP/6-311+G(d,p) level of theory. The BO + H_2 reaction is shown to proceed by abstraction of a hydrogen atom by B to produce OBH + H with the barrier and exothermicity of 8.3 and 6.8 kcal/mol, respectively. The reaction can also occur by 1,2-insertion of BO into the H−H bond or by H abstraction by the O atom; however, the barriers for these channels are much higher, 36.4 and 42.7 kcal/mol, respectively. Via a low ∼0.3 kcal/mol barrier, the OBH + H reaction produces the OBH_2 radical, which is the most stable compound in the BO/H_2 system and lies 15.9, 2.5, and 4.2 kcal/mol below BO + H_2, *trans*-HBOH, and *cis*-HBOH, respectively. OBH_2 can isomerize to *trans*-HBOH overcoming a barrier of 27.7 kcal/mol and the latter can rearrange to the cis conformer with a barrier of 10.8 kcal/mol. BOH and H can recombine and form *cis*- or *trans*-HBOH without barriers. In the B + H_2O reaction, the reactants can first form a weakly bound B−H_2O complex, which then can eliminate an H atom producing BOH + H or undergo insertion of B into an O−H bond giving *trans*-HBOH with barriers of 4.7 and 6.2 kcal/mol relative to the initial reactants, respectively, and *trans*-HBOH can eventually decompose to OBH + H and a minor amount of BO + H_2. Singlet OBBO is shown to be much less reactive with respect to H_2 than the BO monomer. Alternatively, after two BO recombine to form a triplet OBBO molecule over a moderate 8.3 kcal/mol barrier, t-OBBO can easily react with H_2 producing either BO + OBH_2 (via a t-$OBBH_2O$ intermediate) or OBBOH + H with barriers of 4.4 and 7.4 kcal/mol, respectively. The reactions in the BS/H_2 system are shown to be similar to those for BO/H_2, except that BS cannot insert into H_2, SBH_2 resides in a much deeper potential well (37.3 kcal/mol below BS + H_2) and can rearrange both to *trans*- and *cis*-HBSH, the B−H_2S complex is more strongly bound than B−H_2O, and the B + H_2S reaction is expected to be significantly faster than the reaction of B + H_2O.

Introduction

The oxidation of boron to solid or liquid B_2O_3 is a highly exothermic process and therefore boron is of interest as a potential component of propellants.[1−7] However, significant obstacles exist for practical use of elemental boron combustion, including the formation of a protective oxide layer that hinders the ignition of boron particles, the generation of boron oxyhydride intermediates which impede the combustion process, and also a slow condensation rate to the desired liquid or solid final product. When hydrogen is present, a substantial amount of boron gets trapped as metastable species such as HBO and HOBO, with less energy release than would occur with formation of B_2O_3. Because of these problems, extensive efforts are underway to create quantitative models for the complex processes of boron ignition and combustion and to study the detailed kinetics of homogeneous gas-phase[4−6,8] and heterogeneous boron combustion.[5,7] These modeling studies require first of all thermodynamic and kinetic data, including heats of reactions and activation barriers.[9−11] Accurate ab initio and density functional calculations of potential energy surfaces (PES) for the reactions involved in boron combustion are a valuable tool to achieve these data.

In the present paper, we report the results of such calculations for several reactions related to boron combustion. These include various reactions in the BO/H_2 system, such as BO + H_2 → HBO + H, HBO + H → OBH_2/HOBH, and B + H_2O → products. Some of these reactions have been studied earlier experimentally[12−17] and by various theoretical methods;[18−22] however, a complete PES for the BO/H_2 system including all possible intermediates and transition states has not been scrutinized so far at a consistently high level of theory. We also consider the reaction of the boron oxide dimer B_2O_2 with molecular hydrogen and compare its reactivity with that of the monomer. In addition, we study PES and elucidate the gas-phase reaction mechanism of boron sulfide BS with H_2 and compare the BO + H_2 and BS + H_2 reactions. To our knowledge, neither B_2O_2 + H_2 nor BS + H_2 reactions have been studied theoretically until now. The present calculations continue systematic investigations in our group[23−27] of the reactions of diatomic oxides MO and sulfides MS with molecular hydrogen and reverse reactions of atoms with water and H_2S and provide reliable structures of various reactants, products, intermediates, and transition states as well as their energies within chemical accuracy.

Computational Details

We investigate the lowest doublet electronic state PESs for the BO + H_2 → B + H_2O and BS + H_2 → B + H_2S reactions

[†] Tamkang University.
[‡] Florida International University.
[§] Institute of Atomic and Molecular Sciences.

10.1021/jp0357471 CCC: $27.50
Published on Web 12/11/2003

TABLE 1. Total Energies (hartree), ZPE, and Relative Energies (kcal/mol) of Various Compounds in the BO + H_2 Reaction Calculated at the B3LYP/6-311+G(d,p), MP2/6-311G(d,p), CCSD(T)/6-311G(d,p), MP2/6-311+G(3df,2p), and G2M(MP2)// B3LYP/6-311+G(d,p) Levels of Theory

	B3LYP/6-311+G(d,p)			MP2/6-311G(d,p)		CCSD(T)/6-311G(d,p)		MP2/6-311+G(3df,2p)		G2M(MP2)
species	total energy	ZPE	rel energy	total energy	rel energy	total energy	rel energy	total energy	rel energy	rel energy
BO ($C_{\infty v}$, $^2\Sigma^+$)	−100.05887	2.74		−99.80119		−99.81545		−99.85654		
H_2 ($D_{\infty h}$, $^1\Sigma_g^+$)	−1.17957	6.34		−1.16025		−1.16834		−1.16272		
BO + H_2	−101.23844	9.05	0	−100.96144	0	−100.98379	0	−101.01926	0	0
TS1 ($C_{\infty v}$, $^2\Sigma^+$)	−101.23260	8.45	3.08	−100.94554	9.39	−100.96956	8.34	−101.00351	9.29	8.25
H (^{2}S)	−0.50216	0		−0.49981		−0.49981		−0.49981		
OBH ($C_{\infty v}$, $^1\Sigma^+$)	−100.74744	9.01		−100.47875		−100.49552		−100.53581		
OBH + H	−101.24960	9.01	−8.12	−100.97856	−11.86	−100.99533	−7.28	−101.03562	−11.38	−6.81
TS2 (C_s, ^{2}A′)	−101.24856	9.32	−6.09	−100.97851	−10.45	−100.99531	−6.96	−101.03569	−10.05	−6.56
OBH_2 (C_{2v}, $^2B_2$)	−101.28292	12.47	−24.56	−100.97630	−5.97	−101.01571	−16.68	−101.03289	−5.20	−15.90
TS3 (C_s, ^{2}A′)	−101.22942	11.08	7.65	−100.93532	18.38	−100.96249	15.36	−100.99877	14.85	11.82
t-HOBH (C_s, ^{2}A′)	−101.27354	14.94	−16.25	−100.98777	−10.75	−101.01128	−11.47	−101.04859	−12.63	−13.36
TS4 (C_1)	−101.11561	10.81	78.80	−100.82054	90.14	−100.85398	83.18	−100.88062	88.72	81.76
TS5 (C_s, ^{2}A′)	−101.18857	10.74	32.95	−100.90061	39.83	−100.92310	39.74	−100.96384	36.43	36.35
c-HBOH (C_s, ^{2}A′)	−101.27052	14.63	−14.66	−100.98483	−9.21	−101.00819	−9.84	−101.04559	−11.05	−11.68
TS6 (C_1)	−101.25481	13.20	−6.20	−100.96513	1.75	−100.98881	0.92	−101.02847	−1.71	−2.54
TS7 (C_s, ^{2}A′)	−101.17204	7.54	40.19	−100.88243	48.1	−100.91029	44.64	−100.94336	46.15	42.69
BOH (C_s, ^{1}A′)	−100.66957	8.29		−100.39481		−100.42105		−100.45426		
BOH + H	−101.17173	8.29	41.12	−100.89462	41.18	−100.92086	38.74	−100.95407	40.16	37.72
TS8 (C_s, ^{2}A′)	−101.12355	10.49	73.51	−100.82013	90.09	−100.85493	82.27	−100.88116	88.07	80.26
B−H_2O (C_{2v}, $^2B_2$)	−101.13100	14.05	72.32	−100.84153	80.15	−100.87369	73.99	−100.89924	80.22	74.06
B + H_2O	−101.12093	13.36	77.97	−100.83307	84.78	−100.86773	77.06	−100.89332	83.25	75.53
TS9 (C_s, ^{2}A′)	−101.22901	9.60	6.46	−100.93688	15.95	−100.96050	15.15	−100.99657	14.78	13.98

as well as singlet and triplet PESs of the B_2O_2 + H_2 reaction. On these surfaces, full geometry optimizations were run to locate all local minima and transition states at the B3LYP/6-311+G(d,p) level of theory.[28,29] Harmonic vibrational frequencies were obtained at the same level to characterize the stationary points as minima or first-order saddle points, to obtain zero-point vibrational energy corrections (ZPE), and to generate force constant data needed in the intrinsic reaction coordinate (IRC) calculation. To predict more reliable ZPE, the raw calculated B3LYP/6-311+G(d,p) ZPE values were scaled 0.9806 to account for their average overestimation.[30] The IRC method[31] was used to track minimal energy paths from transition structures to corresponding minima. A step size of 0.1 amu$^{1/2}$ bohr or larger was used in the IRC procedure. The relative energies have been refined by using the modified Gaussian-2 G2M(MP2) theory[32] with B3LYP/6-311+G(d,p) optimized geometries. All the ab initio calculations described here were performed employing the Gaussian 98 programs.[33]

Results and Discussion

BO + H_2 → B + H_2O Reaction. Total energies and ZPE corrected relative energies of various compounds in the BO + H_2 → B + H_2O reaction calculated at the B3LYP/6-311+G(d,p), MP2/6-311G(d,p), MP2/6-311+G(3df,2p), and CCSD(T)/6-311G(d,p) levels of theory and their G2M(MP2) relative energies are listed in Table 1. Table 2 presents calculated vibrational frequencies. The BO + H_2 potential energy diagram along the reaction path computed at the G2M(MP2) level and the optimized geometries of various compounds along the predicted reaction pathway are shown in Figure 1.

Three mechanisms are possible in the reaction of boron oxide with molecular hydrogen, including abstraction of an H atom of H_2 by B and O atoms of BO and insertion of boron oxide into the H−H bond. The most favorable mechanism is the abstraction of H by the B atom, BO + H_2 → OBH + H, proceeding via transition state TS1. The barrier for this process is calculated to be 8.3 kcal/mol. The transition state has a linear $C_{\infty v}$-symmetric geometry that ensures the most efficient interaction between the singly occupied σ orbital of BO ($^2\Sigma^+$) composed mostly of the p_z orbital of the boron atom and σ_g and σ_u orbitals of H_2. The resulting OBH molecule is also linear and the BO + H_2 → OBH + H reaction is 6.8 kcal/mol exothermic. In TS1, the breaking H−H bond is stretched by 14% as compared to that in an isolated H_2 molecule, while the forming B−H bond is 35% longer than that in the OBH product. This indicates an early character of the transition state, in line with the finding that the reaction is exothermic. The BO + H_2 → OBH + H reaction has been carefully investigated earlier. The reaction exothermicity was computed to be 6.4, 7.8, and 7.1 kcal/mol at the MRCI/TZ2P,[21] G2,[34] and CBS-Q[35] levels, respectively, all in close agreement with our present value. The reaction barrier obtained by Page using the MRCI/TZ2P method is 9.5 kcal/mol,[21] about 1.2 kcal/mol higher than the G2M(MP2) result.

TABLE 2. Vibrational Frequencies (cm^{-1}) of Various Compounds in the BO + H_2 Reaction Calculated at the B3LYP/6-311+G(d,p) Level

species	frequencies
BO	1916
TS1 (B3LYP)	591*i*, 10, 10, 886, 886, 1885, 2240
TS1 (MP2)[a]	1230*i*, 116, 116, 982, 982, 1758, 2128
OBH	768, 768, 1865, 2902
TS2	375*i*, 268, 762, 784, 1832, 2877
OBH_2	548, 907, 980, 1408, 2425, 2459
TS3	1818*i*, 637, 904, 1419, 2162, 2629
trans-HBOH	748, 870, 1090, 1330, 2574, 3837
TS4	1344*i*, 302, 649, 1084, 2091, 3433
TS5	1681*i*, 868, 985, 1560, 1971, 2130
cis-HBOH	739, 845, 1079, 1341, 2531, 3701
TS6	979*i*, 571, 968, 1301, 2467, 3929
TS7	635*i*, 192, 697, 815, 1468, 2103
BOH	570, 1411, 3816
TS8	1671*i*, 359, 773, 1030, 1384, 3789
B−H_2O	138, 215, 508, 1567, 3660, 3745
TS9	1554*i*, 601, 776, 857, 1666, 2818

[a] Calculated at the MP2/6-311G(d,p) level with the MP2/6-311G(d,p) optimized geometry.

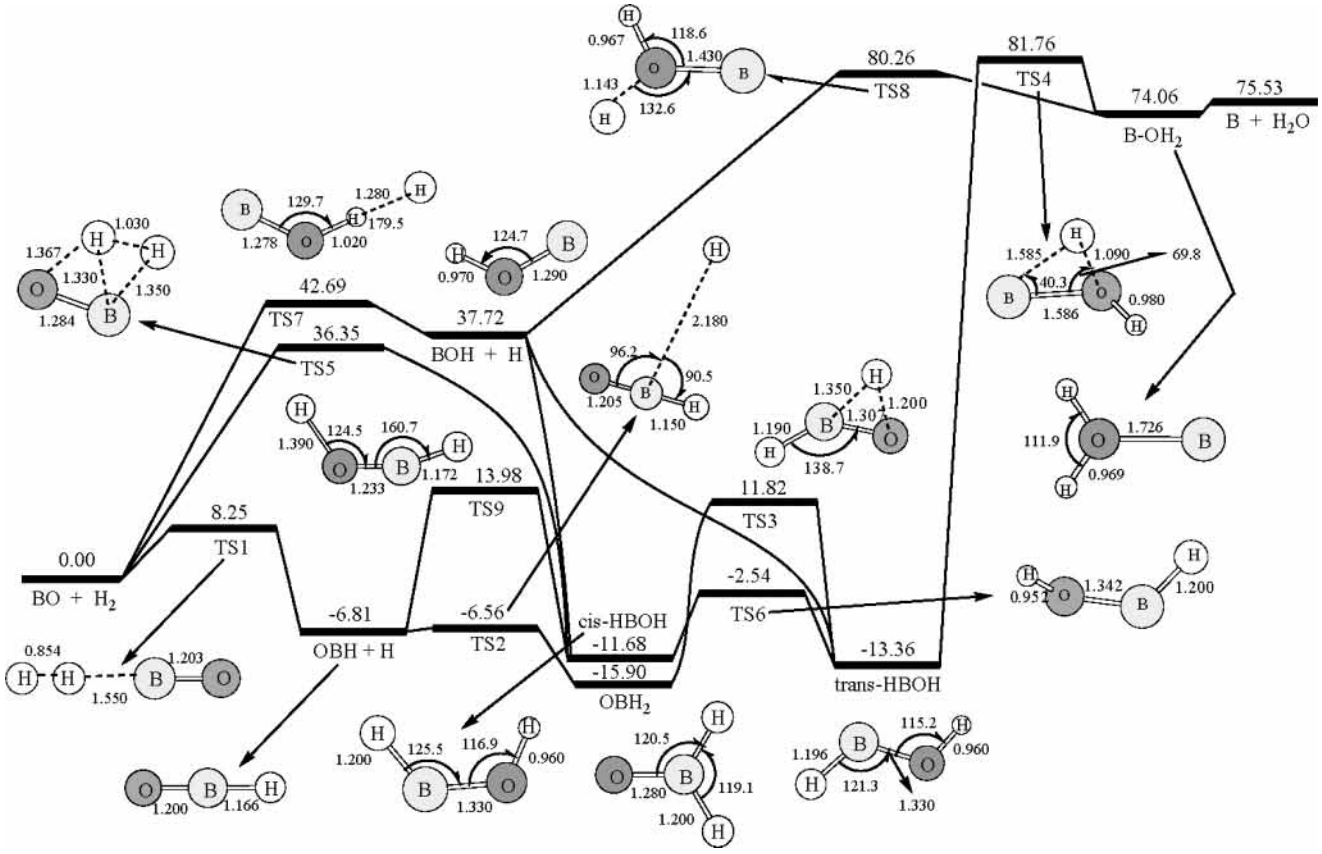

Figure 1. Potential energy diagram for various reactions in the BO/H_2 system calculated at the G2(MP2) level. Relative energies are given in kcal/mol. Geometric structures (bond lengths in Å and bond angles in deg) of various intermediates and transition states optimized at the B3LYP/6-311+G(d,p) level of theory are also shown.

In a secondary OBH + H reaction, the OBH molecule can recombine with H and addition of the latter to the middle B atom is more favorable than the addition to the terminal oxygen. Indeed, the barrier at TS2 for the OBH + H → OBH_2 reaction is only ~0.25 kcal/mol, while that at TS9 for the OBH + H → *cis*-HBOH reaction is 20.5 kcal/mol higher. TS2 has a very early and loose character with the forming B−H bond as long as 2.180 Å. Alternatively, TS9 is a much tighter and later transition state, where the forming O−H bond is only 16% longer than the O−H bond in the *cis*-HBOH product. The C_{2v}-symmetric OBH_2 ($^2B_2$) radical is the global minimum in the BO/H_2 system, which resides 15.9 kcal/mol lower in energy than the initial BO + H_2 reactants. The planar *cis*-HBOH ($^2A'$) isomer is 4.2 kcal/mol less stable than OBH_2 and lies 11.7 kcal/mol below BO + H_2. This value is somewhat lower than the G2 result by Duan et al., 14.0 kcal/mol.[34] The third isomer is planar *trans*-HBOH ($^2A'$), 2.6 kcal/mol less stable than OBH_2 ($^2B_2$) but 1.7 kcal/mol more favorable than *cis*-HBOH ($^2A'$). The energy difference between the *trans*- and *cis*-HBOH conformers computed at the G2 level is very similar, 1.8 kcal/mol.[34] *trans*-HBOH lies 13.4 (G2M(MP2)), 15.8 (G2),[34] and 15.3 (CBS-Q)[35] kcal/mol lower in energy than BO + H_2. It should be noted that we were not able to find a transition state leading directly from OBH + H to *trans*-HBOH; a search of a first-order single point starting from a trans conformation of TS9 converged back to TS9, which connects OBH + H with *cis*-HBOH.

The three isomers of the H_2BO species can rearrange to each other. For instance, migration of a hydrogen atom from B to O in OBH_2 gives *trans*-HBOH via a planar transition state TS3. The barrier at TS3 is significant, 27.7 and 25.2 kcal/mol relative to OBH_2 and *trans*-HBOH, respectively. In turn, *trans*-HBOH can undergo rotation around the B−O bond to produce *cis*-HBOH via an asymmetric transition state TS6. The barrier in this case is much lower, 10.8 and 9.1 kcal/mol relative to *trans*- and *cis*-HBOH, respectively. The B−O bond in HBOH seems to have a single character and the bond elongates only by ~0.01 Å in the transition state. Nevertheless, the barrier at TS6 is rather large for a rotation about an ordinary single bond. Natural bond population analysis for HBOH indicates an additional dative character of the B−O bond with ~0.2 *e* transferred from the p_z lone pair of the oxygen atom to the p_z empty orbital of boron. This dative interaction is upset when the planarity of the molecule is violated, which causes the increase of the barrier. The *trans*-HBOH molecule can eventually dissociate to the B + H_2O products although this reaction is highly endothermic. This process involves two steps, hydrogen transfer from B to O leading to formation of a B−H_2O complex via transition state TS4 and dissociation of the complex occurring without an exit barrier. The barrier at the asymmetric TS4 is 95.1 kcal/mol and the complex resides 87.4 and 74.1 kcal/mol above *trans*-HBOH and BO + H_2, respectively. B−H_2O has a planar C_{2v}-symmetric geometry and $^2B_2$ electronic state and is stabilized only by 1.5 kcal/mol with respect to the boron atom and water molecule. The overall endothermicity of the BO + H_2 → B + H_2O reaction is computed to be 75.5 kcal/mol, close to the experimental value of 76.7 kcal/mol[37] and to the CBS-Q result by Politzer et al., 76.0 kcal/mol.[35]

The second channel of the BO + H_2 reaction proceeds by the 1,2-insertion of BO into the H−H bond of the molecular hydrogen producing the *cis*-HBOH isomer. The reaction barrier at a transition state TS5 is rather high, 36.4 kcal/mol. TS5 has a planar rhomb-shaped structure and $^2A'$ electronic state. Such an arrangement provides an overlap between the singly occupied σ orbital of BO (p_σ on the B atom) and the antibonding vacant

σ_u orbital of H_2 and makes possible the electron density transfer from the former to the latter, which leads to the H−H bond cleavage. Alternatively, we were not able to find a transition state for the 1,1-insertion of the boron atom of BO into H_2 producing OBH_2. If the hydrogen molecule approaches BO within C_{2v} symmetry perpendicularly to the B−O line, the BO ($^2\Sigma^+$) + H_2 ($^1\Sigma_g^+$) → OBH_2 ($^2B_2$) reaction is symmetry forbidden, as the overall wave function of the reactants is $^2A_1$ within the C_{2v} point group. Once symmetry is released, the transition state search converges to the hydrogen abstraction transition state TS1. One can also see that the insertion mechanism leading to *cis*-HBOH is much less favorable than the H-abstraction channel producing OBH + H because the barrier at TS5 is 28.1 kcal/mol higher than that at TS1.

The third, least favorable channel of the BO + H_2 reaction is H-abstraction from H_2 by the oxygen atom of the boron oxide leading to the BOH + H products. The barrier at the corresponding TS7 is computed to be 42.7 kcal/mol and BOH + H lie 37.7 kcal/mol higher in energy than the reactants. The reaction heats computed earlier at the G2 and CBS-Q levels of theory are similar, 37.4 and 38.6 kcal/mol, respectively. In accord with the fact that the reaction is endothermic, TS7 exhibits a late character, with the breaking H−H bond stretched to 1.280 Å, 72% longer than the H−H distance in free H_2, and the forming O−H bond is only 5% longer than that in the BOH product. The BOH angle in TS7 (129.7°) is also rather similar to that in BOH (124.7°), while the OHH fragment is nearly linear. TS7 has a planar geometry and $^2A'$ electronic state. If secondary collisions are possible under the reaction conditions, BOH can easily recombine with H to produce *cis*- or *trans*-HBOH without a barrier. The transition state search for the H atom elimination from B in the two HBOH conformers converged to the BOH + H products thus confirming that the highly exothermic BOH + H → *cis*-HBOH (−49.4 kcal/mol) and BOH + H → *trans*-HBOH (−51.1 kcal/mol) reactions are barrier-free. Finally, the hydrogen atom can also add to the oxygen of BOH to produce the B−H_2O complex. This reaction is 36.3 kcal/mol endothermic and proceeds via a late transition state TS8 over a barrier of 42.5 kcal/mol. Evidently, the BOH + H → B−H_2O → B + H_2O reaction channel is not expected to be competitive with the barrierless H additions forming *cis*- and *trans*-HBOH and with the reverse H abstraction reaction BOH + H → BO + H_2 occurring via a 5.0 kcal/mol barrier.

B + H_2O Reaction. As seen in Figure 1, the B + H_2O reaction can proceed by two different mechanisms following the formation of the weak B−H_2O complex. The first channel leads to *trans*-HBOH over a barrier of 6.2 kcal/mol at TS4. Then, the *trans*-HBOH molecule can isomerize to *cis*-HBOH and the latter would decompose to either OBH + H or BO + H_2. Alternatively, *trans*-HBOH can rearrange to OBH_2 and then dissociate to OBH + H. After TS4 is cleared, all intermediates and transition states lie significantly lower in energy than the B + H_2O reactants. The second channel of the B + H_2O reaction involves elimination of a hydrogen atom via TS8 via a lower 4.7 kcal/mol barrier leading to the BOH + H products. Secondary recombination of BOH and H is most likely to produce chemically activated *cis*- or *trans*-HBOH, which eventually decompose to OBH + H or less probably to BO + H_2. We can expect that the B + H_2O → B−H_2O → TS8 → BOH + H reaction channel is slightly more preferable than B + H_2O → B−H_2O → TS4 → *trans*-HBOH → products (OBH + H or BO + H_2), as the barrier at TS8 is 1.5 kcal/mol lower than that at TS4. Summarizing, we conclude that BOH + H and OBH + H should be major reaction products and a minor amount of BO + H_2 also can be formed. This conclusion qualitatively agrees with that made by Alberti et al. on the basis of their quasiclassical trajectory calculation.[22] If the *trans*- and *cis*-HBOH and OBH_2 intermediates can be stabilized by collisions or in an inert matrix, they can be observed too. In matrix isolation experiments, Jeong et al.[16] identified the HBOH product of the B + H_2O reaction based on the observation of a 1408-cm^{-1} IR band and two weak bands at 2536 and 2571 cm^{-1}. On the other hand, Andrews and Burkholder[17] assigned the major reaction products as HBO and BO. They also observed several absorption peaks between 1408 and 1450 cm^{-1}, but those were assigned to the BOB and OBOB species rather than to HBOH. As seen in Table 2, the 1408-cm^{-1} peak could additionally belong to the IR spectra of BOH or OBH_2, while the bands at 2536 and 2571 cm^{-1} indeed can be due to *cis*- and *trans*-HBOH, respectively. Possibly all of the above-mentioned products were formed in some amounts in the experiments.

There still has been a controversy in the literature of what is the barrier for the B + H_2O reaction. Early MP2/6-31G* calculations by Sakai and Jordan[18] gave the value of ∼12 kcal/mol for the barrier of insertion of B into an O−H bond of H_2O corresponding to our TS4. Alberti et al.[22] used a value of about 20 kcal/mol in their analytical PES employed for the quasiclassical trajectory calculations. On the other hand, more recent B3LYP calculations by Wang and Huang[38] indicated that the insertion barrier is in the range of 0.0 kcal/mol with respect to the initial reactants and the reaction first proceeds via a rather stable B-OH_2 complex, 5.1 kcal/mol below B + H_2O at their best B3LYP/6-311++G(3df,2p) level. Our higher level CCSD(T)/6-311G(d,p) and G2M(MP2) results show that the B + H_2O reaction does have a significant insertion barrier, 6.1−6.2 kcal/mol. Moreover, we demonstrate for the first time that the B + H_2O reaction can directly produce BOH + H through elimination of an H atom from the B−H_2O complex and the H loss barrier is somewhat lower than the insertion barrier.

Rate Constants of the Reactions in the BO/H_2 System. We carried out transition state theory (TST) calculations with Wigner's tunneling corrections[36] of the rate constants for various reactions in the 300−3000 K temperature range:

$$k = \left(\frac{RT}{p^{\circ}}\right)^{-\Delta n^{\ddagger}} \frac{k_B T}{h} e^{-\Delta G_0^{\ddagger}/RT}$$

$$Q_{tun} = 1 - \frac{1}{24}\left(\frac{h\nu_S}{k_B T}\right)^2 (1 + k_B T/E_0)$$

where R is the Rydberg constant, k_B is the Boltzmann constant, h is the Planck constant, T and p° are the temperature and the standard pressure, respectively, $\Delta n^{\ddagger}$ is the change of the number of moles from reactants to the transition state, $\Delta G_0^{\ddagger}$ is the change of the Gibbs free energy from reactants to the transition state, ν_S is the transition state imaginary frequency, and E_0 is the barrier height including ZPE correction. The resultant fitted three-parameter $AT^B\exp(-C/T)$ expressions for the rate constants are collected in Table 3. For the reactions which have a unimolecular character in the forward or reverse direction, the TST rates correspond to the high-pressure limit, while their pressure dependence can be evaluated by using RRKM theory, which is beyond the scope of this paper.

For the BO + H_2 reaction, we compared the calculated rates with those predicted by Page[21] and with available experimental data.[12,13] It should be noted that the B3LYP/6-311+G(d,p) calculations gave a very low value of 10 cm^{-1} for the lowest degenerate vibrational frequency of TS1 (see Table 2). This is

TABLE 3. Fitted Three-Parameter Expressions for Rate Constants of Various Reactions in the BO/H_2 System in the Temperature Range of 300−3000 K

reaction	expression	units
BO + H_2 → TS1 → OBH + H	$2.94 \times 10^{-19}\ T^{2.57} \exp(-2903/T)$	$cm^3\ molecule^{-1}\ s^{-1}$
	$7.49 \times 10^{-23}\ T^{3.53} \exp(-1590/T)$[a]	
OBH + H → TS1 → BO + H_2	$7.01 \times 10^{-16}\ T^{1.77} \exp(-6921/T)$	$cm^3\ molecule^{-1}\ s^{-1}$
OBH + H → TS2 → OBH_2	$2.78 \times 10^{-13}\ T^{1.002} \exp(+159.3/T)$	$cm^3\ molecule^{-1}\ s^{-1}$
OBH + H → TS9 → *cis*-HBOH	$2.78 \times 10^{-14}\ T^{1.10} \exp(-9659/T)$	$cm^3\ molecule^{-1}\ s^{-1}$
OBH_2 → TS2 → OBH + H	$2.43 \times 10^{12}\ T^{0.60} \exp(-5014.5/T)$	s^{-1}
OBH_2 → TS3 → *trans*-HBOH	$2.41 \times 10^{12}\ T^{0.33} \exp(-13652/T)$	s^{-1}
cis-HBOH → TS9 → OBH + H	$3.32 \times 10^{10}\ T^{0.93} \exp(-12590/T)$	s^{-1}
cis-HBOH → TS6 → *trans*-HBOH	$1.46 \times 10^{12}\ T^{0.37} \exp(-4610/T)$	s^{-1}
trans-HBOH → TS3 → OBH_2	$2.39 \times 10^{11}\ T^{0.62} \exp(-12303/T)$	s^{-1}
trans-HBOH → TS6 → *cis*-HBOH	$1.22 \times 10^{12}\ T^{0.41} \exp(-5448/T)$	s^{-1}
trans-HBOH → TS4 → B + H_2O	$2.17 \times 10^{11}\ T^{0.80} \exp(-47784/T)$	s^{-1}
B + H_2O → TS4 → *trans*-HBOH	$1.92 \times 10^{-17}\ T^{2.00} \exp(-2069/T)$	$cm^3\ molecule^{-1}\ s^{-1}$
B + H_2O → TS8 → BOH + H	$7.22 \times 10^{-18}\ T^{2.10} \exp(-1159/T)$	$cm^3\ molecule^{-1}\ s^{-1}$
BOH + H → TS7 → BO + H_2	$4.34 \times 10^{-16}\ T^{1.62} \exp(-1791/T)$	$cm^3\ molecule^{-1}\ s^{-1}$

[a] Recommended expression from ref 12.

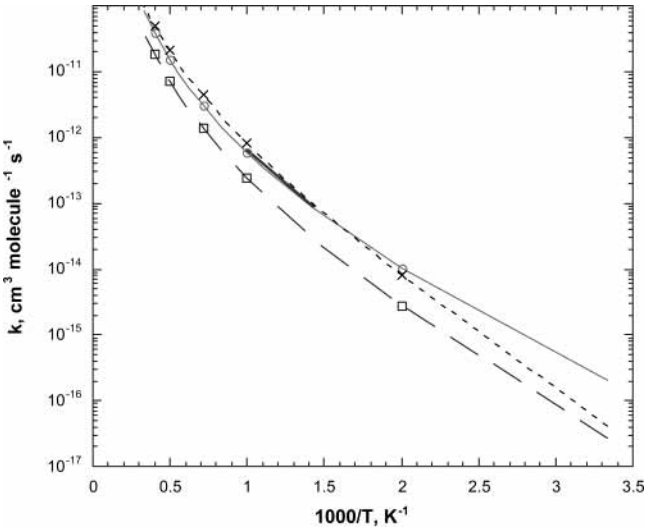

Figure 2. Arrhenius plot of experimental and calculated rate constants for the BO + H_2 → OBH + H reaction. The plain curve marked with open circles shows recommended values from ref 13. The bold line depicts experimental rates from ref 12. The long-dashed (marked with open squares) and short-dashed (marked with "×") curves show theoretical rate constants calculated in ref 21 and in the present work, respectively.

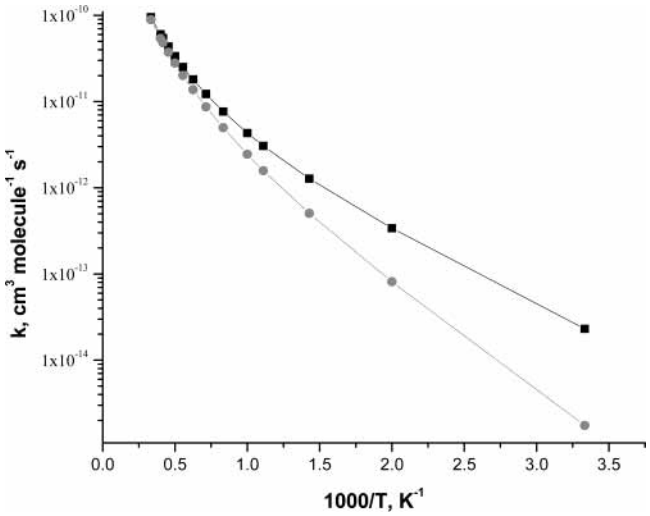

Figure 3. Arrhenius plot of calculated rate constants for the B + H2O → TS8 → BOH + H (marked with solid squares) and B + H2O → TS4 → *trans*-HBOH (marked with solid circles) reactions.

apparently an artifact of the method because TST calculations with this value give an unphysically fast growth of the rate constant with temperature. Hence, we reoptimized the structure and recalculated frequencies of TS1 at the MP2/6-311G(d,p) level. The changes in the optimized bond lengths are small and their effect on the G2M(MP2) energy of TS2 is negligible. As seen in Table 2, the frequency changes are also not very large, except for the lowest degenerate frequency, 116 cm^{-1} at the MP2 level. This seems to be a more reasonable result, although it is somewhat lower than the 173 cm^{-1} obtained by Page at a lower CASSCF(3,3)/DZP level.[21] Therefore, we used the MP2/6-311G(d,p) vibrational frequencies scaled by 0.9496[30] (except for the lowest 116-cm^{-1} frequency which was scaled by 1.0127[30]) to compute the TST rate constants. The results are shown in Figure 2. As one can see, the calculated rates closely agree with recommended rate constants for the 500−3000 K temperature range[13] and with the rates measured experimentally between 690 and 1030 K.[12] The deviation from experiment at low temperatures may be due to small curvature tunneling effects, which are not taken into account in our simple treatment of the tunneling correction. Direct dynamics calculations would be able to provide more accurate rate constants for the low-temperature range. The rates obtained by Page using TST calculations based on his MRCI/TZ2P//CASSCF/DZP PES[21] significantly underestimate experimental and our values, indicating that the reaction barrier is overestimated at that level of theory. Indeed, lowering the calculated barrier from 9.5 to 8.5 kcal/mol and adjustment of the lowest degenerate frequency of the transition state from 173 to 134 cm^{-1} led[12] to excellent agreement between experimental and TST rate constants. Our present higher level calculations confirm this result.

For the B + H2O reaction (see Figure 3), the calculated rate constants indicate that the BOH + H reaction channel occurring via TS8 is faster than the formation of *trans*-HBOH via TS4 for the entire 300−3000 K temperature range. However, the BOH + H/*trans*-HBOH branching ratio decreases from 93/7 at 300 K to 51.6/48.4 at 3000 K.

B_2O_2 + H_2 Reaction. Density functional calculations of PES for the B + H_2O and B_2 + H_2O reactions by Wang and Huang[38] showed that the boron dimer has a higher reactivity than B in inserting into water. In this view, we considered the reaction of the boron oxide dimer with H_2 and compared the reactivity of B_2O_2 with respect to molecular hydrogen with that of BO. The most stable isomer of the boron dimer is linear OBBO, which is 72.3 kcal/mol more stable than a cyclic form at the B3PW91 level.[35] Therefore, we have studied PES of the OBBO

TABLE 4. Total Energies (hartree), ZPE, and Relative Energies (kcal/mol) of Various Compounds in the $B_2O_2 + H_2$ Reaction Calculated at the B3LYP/6-311+G(d,p), MP2/6-311G(d,p), CCSD(T)/6-311G(d,p), MP2/6-311+G(3df,2p), and G2M(MP2)// B3LYP/6-311+G(d,p) Levels of Theory

	B3LYP/6−311+G(d,p)			MP2/6−311G(d,p)		CCSD(T)/6−311G(d,p)		MP2/6−311+G(3df,2p)		G2M(MP2)
species	total energy	ZPE	rel energy	total energy	rel energy	total energy	rel energy	total energy	rel energy	rel energy
s-B_2O_2 ($D_{\infty h}$, $^1\Sigma_g^+$)	−200.30435	8.48		−199.79106		−199.81486		−199.90064		
s-$B_2O_2 + H_2$	−201.48392	14.79	0	−200.95131	0	−200.98320	0	−201.06336	0	0
s-TS1 (C_1)	−201.40964	17.29	49.06	−200.86884	54.19	−200.90120	53.90	−200.98695	50.40	50.10
s-*cis*-OBB(H)OH (C_s, ^{1}A′)	−201.50763	21.77	−8.03	−200.96575	−2.22	−201.00225	−5.12	−201.08262	−5.25	−8.14
s-TS2 (C_1)	−201.48372	20.04	5.27	−200.93747	13.83	−200.97375	11.07	−201.05789	8.58	5.82
s-*trans*-OBB(H)OH (C_s, ^{1}A′)	−201.50657	21.80	−7.34	−200.96451	−1.41	−201.00094	−4.27	−201.08198	−4.81	−7.67
s-TS3 (C_s, ^{1}A′)	−201.40259	17.00	53.21	−200.86153	58.51	−200.89484	57.61	−200.97981	54.60	53.70
s-TS4 (C_s, ^{1}A′)	−201.37208	17.46	72.80	−200.82704	80.60	−200.86060	79.54	−200.94449	77.21	76.15
OBH + OBH	−201.49487	15.82	−5.86	−200.95749	−2.87	−200.99105	−3.92	−201.07161	−4.17	−5.22
t-B_2O_2 (C_s, ^{3}A′)	−200.12818	6.73		−199.59124		−199.63275		−199.70010		
t-$B_2O_2 + H_2$	−201.30775	13.06	108.85	−200.7515	123.69	−200.80109	112.58	−200.86283	124.13	113.03
t-TS1 (C_1)	−201.30623	14.35	111.07	−200.74460	129.28	−200.79474	117.83	−200.85735	128.84	117.39
t-$OBBH_2O$ (C_s, ^{3}A″)	−201.36582	16.12	75.41	−200.79069	102.09	−200.84953	85.18	−200.90026	103.65	86.74
t-TS2 (C_s, ^{3}A″)	−201.34143	15.74	90.34	−200.77661	110.55	−200.83053	96.73	−200.88861	110.58	96.76
BO + OBH_2	−201.34180	15.21	90.23	−200.77749	109.49	−200.83117	95.81	−200.88943	109.56	95.88
t-TS3 (C_s, ^{3}A′)	−201.30376	14.40	112.67	−200.74128	131.41	−200.79061	120.46	−200.85340	131.36	120.42
OBBOH (C_s, ^{2}A′) + H	−201.33840	15.18	91.70	−200.79933	95.75	−200.83219	95.14	−200.91489	93.55	92.94
t-TS4 (C_s, ^{3}A′)	−200.10815	5.83	120.27[a]	−199.58531	126.46[a]	−199.61661	121.75[a]	−199.69763	124.74[a]	120.03[a]

[a] Relative energy is given with respect to s-B_2O_2.

TABLE 5. Vibrational Frequencies (cm^{-1}) of Various Compounds in the $B_2O_2 + H_2$ Reaction Calculated at the B3LYP/ 6-311+G(d,p) Level

species	frequencies
s-B_2O_2	216, 498, 503, 616, 1961, 2135
s-TS1	1816*i*, 193, 240, 495, 518, 675, 979, 1100, 1614, 1982, 2029, 2267
s-*cis*-OBB(H)OH	190, 284, 489, 656, 702, 913, 1005, 1187, 1363, 2010, 2597, 3832
s-TS2	880*i*, 177, 280, 487, 512, 711, 849, 1121, 1315, 1999, 2573, 3993
s-*trans*-OBB(H)OH	175, 285, 503, 671, 701, 891, 1022, 1175, 1346, 2005, 2639, 3836
s-TS3	1887*i*, 184, 187, 374, 473, 692, 790, 992, 1546, 1956, 1976, 2715
s-TS4	1723*i*, 171, 265, 349, 582, 706, 897, 1135, 1605, 1985, 2037, 2481
t-B_2O_2	150, 282, 380, 666, 1289, 1946
t-TS1	301*i*, 140, 156, 229, 306, 389, 494, 627, 671, 1277, 1956
t-$OBBH_2O$	145, 240, 379, 474, 572, 590, 643, 783, 1248, 1983, 2087, 2129
t-TS2	87*i*, 44, 47, 139, 213, 544, 885, 970, 1379, 1913, 2419, 2454
t-TS3	471*i*, 168, 188, 300, 362, 441, 442, 575, 671, 1322, 1967, 3637
OBBOH	176, 206, 279, 458, 611, 988, 1456, 1971, 3677
t-TS4	322*i*, 60, 106, 332, 1683, 1900

$+ H_2$ reaction. The dimer has the $^1\Sigma_g^+$ ground electronic state and is bound by 111.7 kcal/mol (at the G2M(MP2) level) with respect to two monomers.

Total energies and ZPE corrected relative energies of various compounds in the OBBO $+ H_2$ reaction in the ground singlet and lowest triplet electronic states calculated at the B3LYP/6-311+G(d,p), MP2/6-311G(d,p), MP2/6-311+G(3df,2p), and CCSD(T)/6-311G(d,p) levels of theory and their G2M(MP2) relative energies are listed in Table 4, while Table 5 shows calculated vibrational frequencies. The OBBO $+ H_2$ potential energy diagram along the reaction path computed at the G2M-(MP2) level and the optimized geometries of various compounds along the predicted reaction pathways are shown in Figure 4. In accord with its higher stability as compared to BO, OBBO exhibits a lower reactivity. We found two channels for the OBBO $+ H_2$ reaction. The first mechanism is 1,2-insertion of a BO fragment into the H−H bond proceeding via transition state s-TS1 via a barrier of 50.1 kcal/mol. This process leads to a *cis*-OBB(H)OH intermediate residing 8.1 kcal/mol below the reactants. As one can see, the 1,2-insertion barrier for OBBO is 13.8 kcal/mol higher than that for the BO monomer. Next, *cis*-OBB(H)OH can isomerize to a trans conformer by rotation around the B−O bond. The calculated barrier is 14.0 kcal/mol and it occurs at s-TS2. The *trans*-OBB(H)OH isomer lies 0.5 kcal/mol higher in energy than the cis form. *trans*-OBB(H)OH can dissociate to two OBH molecules through 1,2-hydrogen migration from one boron atom to the other accompanied by a cleavage of the B−B bond. The corresponding transition state s-TS3 lies 53.7 and 61.4 kcal/mol above OBBO $+ H_2$ and *trans*-OBB(H)OH, respectively. The overall exothermicity of the OBBO $+ H_2 \rightarrow$ 2OBH is calculated to be 5.2 kcal/mol at the G2M(MP2) level, somewhat higher than the CBS-Q value of 2.3 kcal/mol.[35] Otherwise, *cis*- and *trans*-OBB(H)OH can decompose to OBBOH + H or BO + OBH_2 by the cleavage of the B−H or B−B single bonds, respectively. However, these processes are highly endothermic, as the products reside 92.9 (OBBOH + H) and 95.9 kcal/mol (BO + OBH_2) higher in energy than OBBO $+ H_2$.

The alternative reaction channel is 1,2-insertion of the B−B fragment of OBBO into the H_2 molecule. This leads directly to the OBH + OBH products; two new B−H bonds are formed, while the H−H and B−B bonds are cleaved during this process occurring via transition state s-TS4. The barrier is very high, 76.1 kcal/mol, so that this reaction mechanism is not likely. As was described in a previous section, the most favorable mechanism of the BO $+ H_2$ reaction is H abstraction leading

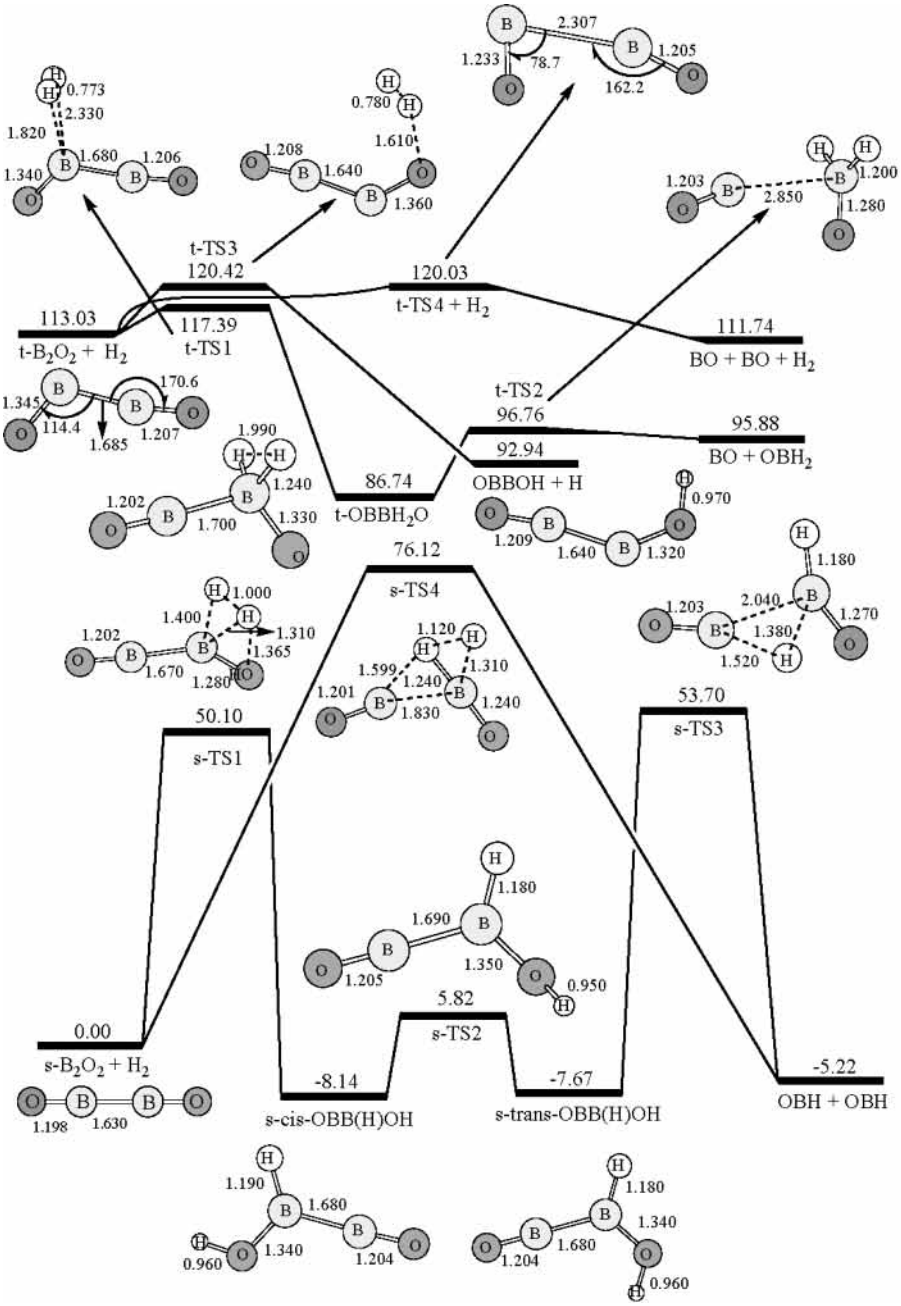

Figure 4. Potential energy diagram for the $B_2O_2 + H_2$ reactions in the lowest singlet and triplet electronic states calculated at the G2(MP2) level. Relative energies are given in kcal/mol. Geometric structures (bond lengths in Å and bond angles in deg) of various intermediates and transition states optimized at the B3LYP/6-311+G(d,p) level of theory are also shown.

to OBH + H. In the case of OBBO, the hydrogen abstraction would lead from two closed-shell species to two radicals, OBBOH + H. Therefore, the reaction energy, 92.9 kcal/mol, is too high and this channel is not probable. As a consequence of its greater stability, the singlet OBBO is not expected to be reactive with molecular hydrogen, except at high temperatures when the 50.1 and 53.7 kcal/mol at s-TS1 and s-TS3 can be overcome and two OBH molecules can be produced.

Alternatively, electronically excited triplet OBBO, which lies 113.0 kcal/mol above the ground state minimum and 1.7 kcal/mol higher in energy than two BO monomers, can easily react with H_2. The most favorable reaction mechanism is 1,1-insertion of a B atom into the H−H bond proceeding via transition state t-TS1 with a barrier of 4.4 kcal/mol. The transition state has an asymmetric geometry and a very early character (see Figure 4). A t-$OBBH_2O$ molecule residing 26.3 kcal/mol below t-B_2O_2 + H_2 is formed as a result of the insertion. This molecule can decompose to the BO + OBH_2 products via a barrier of 10.0 kcal/mol at t-TS2. The transition state lies 16.3 kcal/mol lower in energy than the initial triplet state reactants, so that the decomposition of the chemically activated t-$OBBH_2O$ species is expected to be fast. The t-$B_2O_2 + H_2 \rightarrow$ BO + OBH_2 reaction is thus 17.2 kcal/mol exothermic and the initial step with the 4.4 kcal/mol barrier is rate determining. The second channel of the t-$B_2O_2 + H_2$ reaction involves abstraction of a hydrogen atom by a terminal oxygen. In this case, the products are OBBOH + H and the reaction is more exothermic, by 20.1 kcal/mol. However, the abstraction barrier located at t-TS3, 7.4 kcal/mol, is 3.0 kcal/mol higher than the insertion barrier at t-TS1. Therefore, the production of BO + OBH_2 in the reaction of the triplet boron dimer with molecular hydrogen is expected to be more probable than the production of OBBOH + H.

TABLE 6. Total Energies (hartree), ZPE, and Relative Energies (kcal/mol) of Various Compounds in the BS + H_2 Reaction Calculated at the B3LYP/6-311+G(d,p), MP2/6-311G(d,p), CCSD(T)/6-311G(d,p), MP2/6-311+G(3df,2p), and G2M(MP2)// B3LYP/6-311+G(d,p) Levels of Theory

	B3LYP/6-311+G(d,p)			MP2/6-311G(d,p)		CCSD(T)/6-311G(d,p)		MP2/6-311+G(3df,2p)		G2M(MP2)
species	total energy	ZPE	rel energy	total energy	rel energy	total energy	rel energy	total energy	rel energy	rel energy
BS ($C_{\infty v}$, $^2\Sigma^+$)	−423.00362	1.68		−422.35806		−422.38860		−422.41142		
BS + H_2	−424.18319	8.00	0	−423.51831	0	−423.55694	0	−423.57414	0	0
TS1 ($C_{\infty v}$, $^2\Sigma^+$)	−424.17527	7.12	4.11	−423.50101	10.00	−423.54029	9.59	−423.55800	9.27	8.86
SBH ($C_{\infty v}$, $^1\Sigma^+$)	−423.68919	7.82		−423.03345		−423.06494		−423.09019		
SBH + H	−424.19135	7.82	−5.29	−423.53326	−9.56	−423.56475	−5.08	−423.59000	−10.13	−5.65
TS2 (C_s, $^2A'$)	−424.19138	8.00	−5.14	−423.53174	−8.43	−423.56352	−4.13	−423.58897	−9.31	−5.01
SBH_2 (C_{2v}, $^2B_2$)	−424.25794	12.23	−42.77	−423.58283	−36.34	−423.62329	−37.49	−423.63829	−36.12	−37.26
TS3 (C_s, $^2A'$)	−424.19026	9.72	−2.75	−423.51799	1.89	−423.55607	2.24	−423.57761	−0.49	−0.14
trans-HBSH (C_s, $^2A'$)	−424.21860	11.76	−18.53	−423.55051	−16.52	−423.58820	−15.95	−423.60803	−17.58	−17.00
TS4 (C_1)	−424.08540	8.36	61.71	−423.40653	70.49	−423.45637	63.46	−423.46236	70.49	63.46
TS9 (C_s, $^2A'$)	−424.18932	8.10	−3.75	−423.52211	−2.29	−423.55631	0.49	−423.58020	−3.71	−0.92
cis-HBSH (C_s, $^2A'$)	−424.21860	11.76	−18.53	−423.54837	−15.17	−423.58618	−14.66	−423.60600	−16.30	−15.79
TS6 (C_1)	−424.19273	10.62	−3.42	−423.52185	0.35	−423.55954	0.94	−423.57954	−0.82	−0.23
TS5 (C_s, $^2A'$)	−424.18074	9.90	3.40	−423.50508	10.17	−423.54475	9.52	−423.56641	6.72	6.07
TS7 (C_s, $^2A'$)	−424.08401	5.86	60.13	−423.41708	61.42	−423.46036	58.50	−423.47437	60.51	57.59
BSH (C_s, $^1A'$)	−423.58157	5.67		−422.92110		−422.96386		−422.97749		
BSH + H	−424.08372	5.67	60.13	−423.42091	58.84	−423.46367	56.24	−423.47730	58.48	55.89
TS8 (C_1)	−424.08102	6.57	62.70	−423.40018	72.72	−423.45197	64.46	−423.45752	71.77	63.52
B−H_2S (C_{2v}, $^2B_2$)	−424.09464	9.75	57.28	−423.41589	65.99	−423.46486	59.50	−423.47517	63.83	57.34
B + H_2S	−424.08500	9.41	63.00	−423.41560	65.84	−423.46365	59.92	−423.46810	67.92	62.01

Interestingly, the presence of a second BO radical can alter the course of the BO + H_2 reaction. For instance, two BO radicals can recombine to form triplet OBBO via a barrier of 8.3 kcal/mol at t-TS4 (see Figure 4). The recombination on the triplet PES is certainly less favorable than the 111.7 kcal/mol exothermic and barrierless formation of s-OBBO in the singlet electronic state; however, the triplet reaction can play some role at elevated and high temperatures. Then, t-B_2O_2 can react with H_2 by the following mechanism, t-B_2O_2 + H_2 → t-TS1 → t-$OBBH_2O$ → t-TS2 → BO + OBH_2. The overall reaction is then BO + BO + H_2 → BO + OBH_2 and the rate-limiting step is the initial recombination of two BO with the barrier of 8.3 kcal/mol. Without a second BO, the BO + H_2 reaction produces OBH + H with a similar barrier. Thus, the second boron oxide species can enhance the formation of the OBH_2 radical instead of HBO + H.

BS + H_2 → B + H_2S Reaction. Total energies and ZPE corrected relative energies of various compounds in the BS + H_2 → B + H_2S reaction calculated at the B3LYP/6-311+G(d,p), MP2/6-311G(d,p), MP2/6-311+G(3df,2p), and CCSD(T)/6-311G(d,p) levels of theory and their G2M(MP2) relative energies are collected in Table 6. Table 7 shows calculated vibrational frequencies. The BS +H_2 potential energy diagram along the reaction path computed at the G2M(MP2) level and the optimized geometries of various compounds along the predicted reaction pathway are shown in Figure 5. The mechanism of the BS + H_2 reaction is similar to that for BO + H_2, although the energetics and some details differ. Hence, we used the same notation for transition states in the BS/H_2 system as that for BO/H_2.

The most favorable reaction channel is abstraction of a hydrogen atom of H_2 by a B atom of BS, giving the SBH + H products. The calculated barrier at the linear transition state TS1 and the reaction exothermicity, 8.9 and 5.7 kcal/mol, respectively, are very close to the values obtained for the BO + H_2 → OBH + H_2 reaction. As compared to BO + H_2, the reaction exothermicity decreases by 1.1 kcal/mol and the barrier correspondingly increases by 0.6 kcal/mol. In the secondary SBH + H reaction, the hydrogen atom can easily add to the middle boron of SBH to produce the SBH_2 molecule. The barrier at TS2 is only 0.6 kcal/mol, slightly higher than the 0.3 kcal/mol calculated for the OBH + H → OBH_2 process. However, SBH_2 is more stable than OBH_2 because the former resides 37.3 kcal/mol lower in energy than BS + H_2 as compared to only 15.9 kcal/mol for the latter. The addition of H to the sulfur end of SBH forming *cis*-HBSH via TS9 exhibits a somewhat higher barrier, 4.7 kcal/mol. This value is much lower than the barrier for the OBH + H → TS9 → *cis*-HBOH process, 20.8 kcal/mol. *cis*-HBSH lies 15.8 kcal/mol below BS + H_2, i.e., it is slightly more stable than *cis*-HBOH with respect to BO + H_2, −11.7 kcal/mol. The *trans*-HBSH isomer is 1.2 kcal/mol more stable than the cis conformer, but 20.3 kcal/mol less favorable than SBH_2. One can see that the SBH_2 structure lies in a deeper potential energy well with respect to the HBSH isomers as compared to OBH_2. 1,2-Hydrogen migration from B to S via TS3 leads from SBH_2 to *trans*-HBSH but the barrier is higher than that in the BO/H_2 system, 37.1 versus 27.7 kcal/mol. The rotational barrier at TS6 separating the trans and cis forms of HBSH is calculated to be 16.8 and 15.6 kcal/mol relative to *trans*- and *cis*-HBSH, respectively, again higher than the rotational barrier for HBOH, 10.8 and 9.1 kcal/mol. The increase of the barrier for the rotation around the B−S bond correlates

TABLE 7. Vibrational Frequencies (cm^{-1}) of Various Compounds in the BS + H_2 Reaction Calculated at the B3LYP/6-311+G(d,p) Level

species	frequencies
TS1 (B3LYP)	767*i*, 25, 25, 925, 925, 1171, 1934
TS1 ((MP2)[a]	1331*i*, 58, 58, 924, 924, 1177, 1913
SBH	723, 723, 1186, 2839
TS2	136*i*, 139, 719, 720, 1176, 2840
SBH_2	564, 837, 893, 1103, 2538, 2615
TS3	1449*i*, 444, 764, 885, 2045, 2664
trans-HBSH	597, 681, 840, 919, 2500, 2690
TS4	428*i*, 222, 260, 945, 1746, 2670
TS9	481*i*, 265, 680, 722, 1156, 2841
cis-HBSH	597, 681, 840, 919, 2500, 2690
TS6	1157*i*, 602, 755, 830, 2604, 2640
TS5	1226*i*, 604, 738, 899, 1954, 2732
TS7	263*i*, 134, 306, 631, 751, 2276
BSH	602, 760, 2545
TS8	529*i*, 169, 382, 673, 723, 2647

[a] Calculated at the MP2/6-311G(d,p) level with the MP2/6-311G(d,p) optimized geometry.

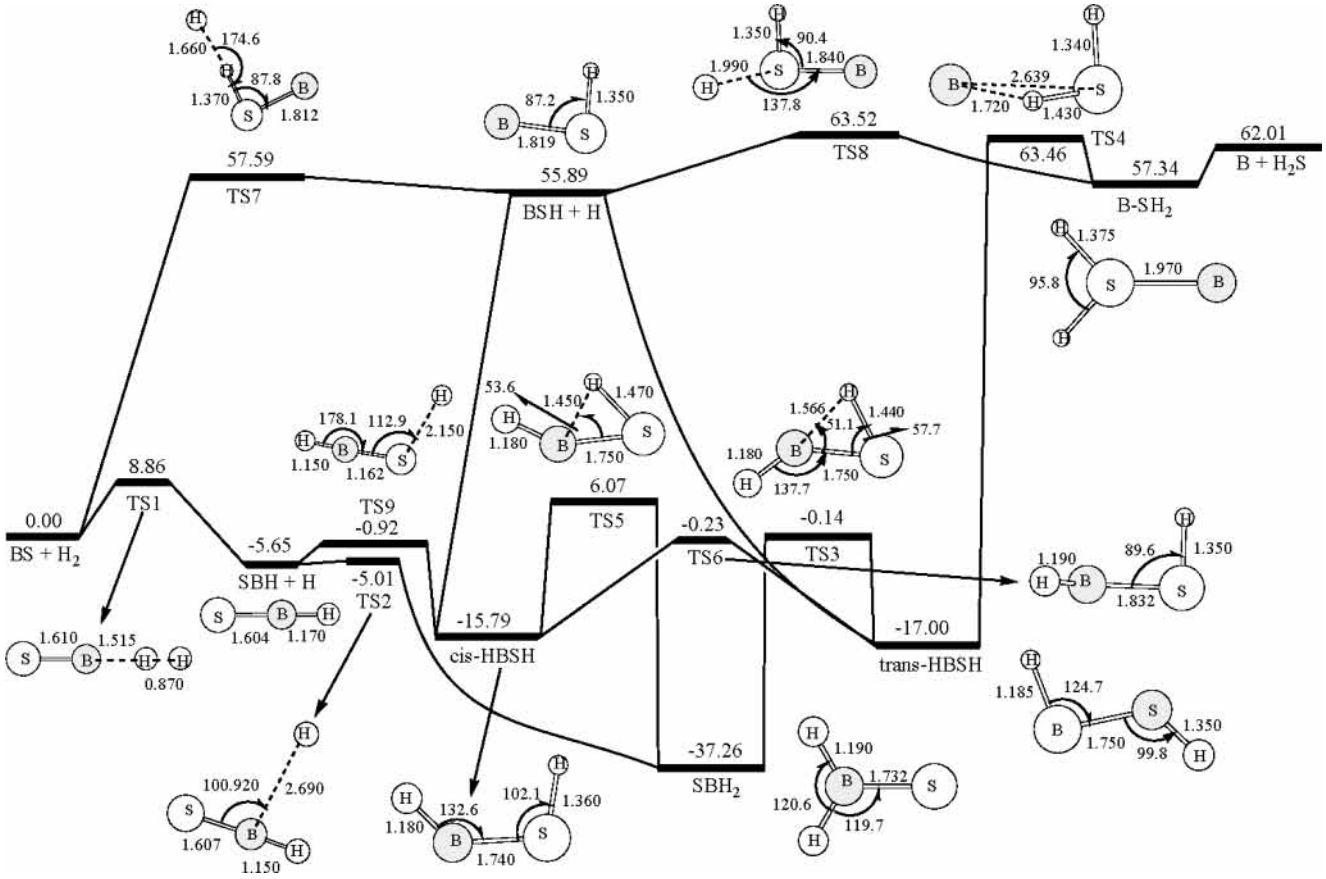

Figure 5. Potential energy diagram for various reactions in the BS/H_2 system calculated at the G2(MP2) level. Relative energies are given in kcal/mol. Geometric structures (bond lengths in Å and bond angles in deg) of various intermediates and transition states optimized at the B3LYP/6-311+G(d,p) level of theory are also shown.

with larger elongation of the B−S bond in TS6, 0.08−0.09 Å, as compared to only 0.01 Å in HOBH.

In addition to TS3, the transition state between SBH_2 and *trans*-HBSH, we also found a transition state connecting SBH_2 with the *cis*-HBSH isomer. We started the first-order saddle point search with a structure similar to TS5 for BO/H_2, which is a transition state for 1,2-insertion of BO into the H−H bond. However, the calculations converged to the structure TS5 shown in Figure 5, which, according to IRC calculations, connects *cis*-HBSH with SBH_2 but not with BS + H_2. This result represents the main difference between the BS/H_2 and BO/H_2 systems. Thus, on the contrary to BO, boron sulfide cannot insert into the H−H bond of H_2. As we discussed above, the 1,1-insertion is not favorable because the singly occupied p_z orbital of the boron atom cannot interact in this case both with the occupied σ_g and vacant σ_u orbitals of H_2. A first-order saddle point on the 1,2-insertion pathway disappears for BS apparently because of a larger size of the BS molecule as compared to BO. Along this pathway, the H−H bond has to be broken and S−H to be formed while the electron density is transferred from p_z(B) to $\sigma_u(H_2)$. The B−S bond length is ∼0.4 Å longer than B−O and the H−H bond has to be stretched more significantly before the S−H bond can start to form, which leads to an energy increase on the insertion pathway. On the other hand, in *cis*-HBSH two hydrogen atoms are located farther away from each other than in *cis*-HBOH and repulsion between them is not as large when one of them migrates from S to B, making possible the direct *cis*-HBSH → SBH_2 rearrangement. In HBOH, two hydrogens have to be located in a trans position to allow the 1,2-H shift.

The barrier at TS5 is calculated to be 21.9 kcal/mol relative to *cis*-HBSH, 5.0 kcal/mol higher than the barrier for the *trans*-HBSH → SBH_2 isomerization at TS3. The HBSH species can decompose to BSH + H without exit barriers and the strengths of the B−H bond are 71.7 and 72.9 kcal/mol for the cis and trans isomers, respectively. Additionally, *trans*-HBSH can dissociate to B + H_2S through a 1,2-H shift from B to S and formation of the B−H_2S complex. Note that the B−H_2S complex formation energy, 4.7 kcal/mol, is significantly larger than that for B−H_2O, 1.5 kcal/mol. The overall heat of the endothermic BS + H_2 → B + H_2S reaction, 62.0 kcal/mol, is 13.5 kcal/mol lower than the endothermicity of the BO + H_2 → B + H_2O reaction.

Since the insertion of BS into H−H is not possible, the only alternative channel of the BS + H_2 reaction is H abstraction by the S atom leading to BSH + H. As for BO + H_2, the BS + H_2 → BSH + H reaction is endothermic and exhibits a high barrier at TS7. The barrier height and reaction heat, 57.6 and 55.9 kcal/mol, respectively, both are 14.9 and 18.2 kcal/mol higher than the corresponding values for the BO + H_2 → BOH + H reaction. BSH and H can in turn recombine producing *cis*- or *trans*-HBSH without entrance barriers. The reverse BSH + H → BS + H_2 abstraction reaction has a 1.7-kcal/mol barrier, 3.3 kcal/mol lower than that for BOH + H → BO + H_2. Finally, H addition to the S atom of BSH gives the B−SH_2 complex via a barrier of 7.6 kcal/mol at TS8. This barrier is much lower than the barrier calculated for the BOH + H → TS8 → B−OH_2 process, 42.5 kcal/mol.

The B + H_2S reaction starts from the formation of the relatively strong B−SH_2 complex and then proceeds by elimina-

TABLE 8. Calculated and Experimental Heats of Formation [ΔH_f(0K), kcal/mol] for Various Species in the BO/H_2, B_2O_2/H_2, and BS/H_2 Systems

species	calcd[a]	exptl	G3[b]	CBS-Q[b]
BO	1.2	1.6 ± 2.6[c]	0.8	1.6
OBH	−57.2	-50.2 ± 6.0[c]	−57.6	−57.6
BOH	−12.7			
OBH_2	−14.7			
trans-HBOH	−12.2			
cis-HBOH	−10.5			
B*2O2*	−109.3	-109.9 ± 2.4[c]	−112.4	−112.4
cis-OBB(H)OH	−117.4			
trans-OBB(H)OH	−117.0			
BS	67.6	57.4 ± 4.1[d]	66.5	66.5
SBH	10.3	−4.0[d]	10.1	10.1
BSH	71.8			
SBH_2	30.3			
trans-HBSH	50.6			
cis-HBSH	51.8			

[a] Present calculations. Based on the heats of reactions calculated in this study and experimental ΔH_f(0K) for B (133.8 kcal/mol), H_2O (−57.1), H_2S (−4.2), and H (51.6). [b] Theoretical data obtained with use of the G3 and CBS-Q methods are taken from ref 40. [c] From ref 39. [d] From ref 37.

tion of an H atom via a barrier of only 1.5 kcal/mol with respect to the initial reactants leading to the BSH + H products. On the other hand, B can insert into an S−H bond and produce *trans*-HBSH with a barrier of 1.45 kcal/mol relative to B + H_2S. Then, *trans*-HBSH can rearrange to SBH_2 or *cis*-HBSH via transition states lying much lower in energy than the reactants. As HBSH and SBH_2 can decompose only SBH + H (not counting highly endothermic dissociation to BSH + H, which more likely can be formed by the H elimination mechanism from the B−SH_2 complex), BS + H_2 cannot be primary products of the B + H_2S reaction. This is an implication of the fact that no transition state exists for the insertion of BS into H_2. As compared to the B + H_2O reaction, B + H_2S is expected to be much faster because the activation barriers are as low as 1.5 kcal/mol, significantly lower than 4.7 and 6.2 kcal/mol for B + H_2O.

Heats of Formation for Various Species. Heats of formation of various species in the BO/H_2, B_2O_2/H_2, and BS/H_2 systems computed by using the heats of reactions calculated in the present study are collected in Table 8. They are compared with available experimental data[37,39] and with the results of most accurate theoretical calculations, using the G3 and CBS-Q model chemistries.[40] As one can see, the agreement of the calculated ΔH_f with experiment is within 1 kcal/mol for BO and B_2O_2. On the other hand, the deviations are large for OBH (7 kcal/mol), BS (10 kcal/mol), and SBH (14 kcal/mol). However, our results for these species closely agree with the values obtained at the most accurate G3 and CBS-Q levels of theory. As the experimental ΔH_f values for OBH, BS, and SBH were reported[40] with large error bars and are not well established, new measurements would be required to reconcile theory and experiment. For the reaction intermediates, such various isomers of OBH_2, SBH_2, and $B_2O_2H_2$, experimental heats of formation are not available to our knowledge, and our calculations provide these important thermodynamic quantities.

Conclusions

G2M(MP2) calculations of PES for the BO + H_2 reaction demonstrate that the reaction proceeds by abstraction of a hydrogen atom by B of the boron oxide to produce OBH + H and the barrier and exothermicity of the reaction are computed to be 8.3 and 6.8 kcal/mol, respectively. TST calculations of the reaction rate constants with the G2M(MP2) barrier and MP2/6-311G(d,p) vibrational frequencies of the transition state give close agreement with experiment for the rates in the 500−3000 K temperature range. The reaction can also occur by 1,2-insertion of BO into the H−H bond or by H abstraction by the O atom; however, the barriers for these mechanisms are much higher, 36.4 and 42.7 kcal/mol, respectively. The OBH + H reaction produces the OBH_2 radical via a small ∼0.3-kcal/mol barrier. OBH_2 is 2.5 and 4.2 kcal/mol lower in energy than *trans*- and *cis*-HBOH, respectively, and can isomerize to *trans*-HBOH by the 1,2-H shift overcoming a barrier of 27.7 kcal/mol. In turn, *trans*-HBOH can rearrange to the cis conformer by rotation about the B−O bond over a barrier of 10.8 kcal/mol. Dissociation of *trans*-HBOH to B + H_2O is highly endothermic and is not probable. BOH and H can recombine and form *cis*- or *trans*-HBOH without barriers. In the B + H_2O reaction, the reactants can first form a weakly bound B−H_2O complex, which then can eliminate an H atom producing BOH + H over a barrier of 4.7 kcal/mol with respect to the initial reactants. The second channel is insertion of B into an O−H bond giving *trans*-HBOH via a 6.2-kcal/mol barrier. The most probable products for this channel are OBH + H, although minor amounts of BO + H_2 and BOH + H also can be produced.

If two BO radicals form a stable dimer OBBO in the ground singlet electronic state, the reactivity with respect to molecular hydrogen drastically decreases because the barriers for the OBBO + H_2 → *cis*-OBB(H)OH → *trans*-OBB(H)OH → OBH + OBH reaction are calculated to be as high as 50−54 kcal/mol. Alternatively, two BO can recombine to form the OBBO molecule in triplet electronic state over a moderate 8.3-kcal/mol barrier. t-OBBO can easily react with H_2 producing either BO + OBH_2 (via a t-$OBBH_2O$ intermediate) or OBBOH + H with barriers of 4.4 and 7.4 kcal/mol, respectively. Thus, the formation of the triplet dimer can enhance the yield of OBH_2.

The reactions in the BS/H_2 system are shown to be similar to those for BO/H_2, except for some details in the energetics and mechanism. The main differences are that BS cannot insert into H_2 and SBH_2 resides in a much deeper potential well (37.3 kcal/mol below BS + H_2) and rearranges by 1,2-H migrations not only to *trans*- but also to *cis*-HBSH. B and H_2S can form a much more strongly bound complex than B and H_2O and the B + H_2S reaction is expected to be significantly faster than B + H_2O because the barriers for H elimination from the complex and for B insertion into an S−H bond are in the range of 1.5 kcal/mol. BSH + H and SBH + H are predicted to be produced in the B + H_2S reaction, while BS + H_2 are not likely to be formed as primary products.

Acknowledgment. This work was supported by the National Science Council of Taiwan, R.O.C. Partial support from Academia Sinica and Tamkang University is also appreciated. A.M.M. is thankful to Florida International University for his start-up funds used to purchase the computer equipment partially employed for this study.

References and Notes

(1) Burdette, C. W.; Lander, H. R.; McCoy, J. R. *J. Energy* **1978**, *2*, 289.

(2) Turns, S. R.; Holl, J. T.; Solomon, A. S. P.; Faeth, G. M. *Combust. Sci. Technol.* **1985**, *43*, 287.

(3) Yetter, R. A.; Cho, S. Y.; Rabitz, H.; Dryer, F. L.; Brown, R. C.; Kolb, C. E. In *22nd Symposium (International) on Combustion*; The Combustion Institute: Pittsburgh, PA, 1988; p 919.

(4) Yetter, R. A.; Rabitz, H.; Dryer, F. L.; Brown, R. C.; Kolb, C. E. *Combust. Flame* **1991**, *83*, 43.

(5) Brown, R. C.; Kolb, C. E.; Rabitz, H.; Cho, S. Y.; Yetter, R. A.; Dryer, F. L. *Int. J. Chem. Kinet.* **1991**, *23*, 957.
(6) Pasternack, L. *Combust. Flame* **1992**, *90*, 259.
(7) Brown, R. C.; Kolb, C. E.; Cho, S. Y.; Yetter, R. A.; Dryer, F. L.; Rabitz, H. *Int. J. Chem. Kinet.* **1994**, *26*, 319.
(8) Brown, R. C.; Kolb, C. E.; Cho, S. Y.; Yetter, R. A.; Dryer, F. L. In *Gas-Phase Metal Reaction*; Fontijn, A., Ed.; Elsevier: Amsterdam, The Netherlands, 1992; p 647.
(9) Brown, R. C.; Kolb, C. E.; Yetter, R. A.; Dryer, F. L.; Rabitz, H. *Combust. Flame* **1995**, *101*, 221.
(10) Yetter, R. A.; Dryer, F. L.; Rabitz, H.; Brown, R. C.; Kolb, C. E. *Combust. Flame* **1998**, *112*, 387.
(11) Zhou, W.; Yetter, R. A.; Dryer, F. L.; Rabitz, H.; Brown, R. C.; Kolb, C. E. *Combust. Flame* **1998**, *112*, 507.
(12) Garland, N. L.; Stanton, C. T.; Nelson, H. H.; Page, M. *J. Chem. Phys.* **1991**, *95*, 2511.
(13) Garland, N. L. In *Gas-Phase Metal Reaction*; Fontijn, A., Ed.; Elsevier: Amsterdam, The Netherlands, 1992; p 73.
(14) Gole, J. L.; Pace, S. A. *J. Phys. Chem.* **1981**, *85*, 2651.
(15) DiGiuseppe, T. G.; Estes, R.; Davidovits, P. *J. Phys. Chem.* **1982**, *86*, 260.
(16) Jeong, G. H.; Boucher, R.; Klabunde, K. J. *J. Am. Chem. Soc.* **1990**, *112*, 3332.
(17) Andrews, L.; Burkholder, T. R. *J. Phys. Chem.* **1991**, *95*, 8554.
(18) Sakai, S.; Jordan, K. D. *J. Phys. Chem.* **1983**, *87*, 2293.
(19) Sakai, S.; Jordan, K. D. *Chem. Phys. Lett.* **1986**, *130*, 103.
(20) Alberti, M.; Sayos, R.; Gonzalez, M.; Gimenez, M.; Bofill, J.; Aguilar, A. *J. Mol. Struct. (THEOCHEM)* **1988**, *166*, 301.
(21) Page M. *J. Phys. Chem.* **1989**, *93*, 3639.
(22) Alberti, M.; Sayos, R.; Sole, A.; Aguilar, A. *J. Chem. Soc., Faraday Trans.* **1991**, *87*, 1057.
(23) Hwang, D.-Y.; Mebel, A. M. *Chem. Phys. Lett.* **2000**, *321*, 95.
(24) Hwang, D.-Y.; Mebel, A. M. *J. Am. Chem. Soc.* **2000**, *122*, 11407.
(25) Hwang, D.-Y.; Mebel, A. M. *Chem. Phys. Lett.* **2001**, *341*, 393.
(26) Mebel, A. M.; Hwang, D.-Y. *J. Phys. Chem. A* **2001**, *105*, 7460.
(27) Hwang, D.-Y.; Mebel, A. M. *J. Phys. Chem. A* **2002**, *106*, 520.
(28) Becke, A. D. *J. Chem. Phys.* **1993**, *98*, 5648.
(29) Lee, C.; Yang, W.; Parr, R. G. *Phys. Rev. B* **1988**, *37*, 785.
(30) Scott, A. P.; Radom, L. *J. Phys. Chem.* **1996**, *100*, 16512.
(31) Gonzalez, C.; Schlegel, H. B. *J. Phys. Chem.* **1990**, *94*, 5523.
(32) Mebel, A. M.; Morokuma, K.; Lin, M. C. *J. Chem. Phys.* **1995**, *103*, 7414.
(33) Frisch, M. J.; Trucks, G. W.; Schlegel, H. B.; Scuseria, G. E.; Robb, M. A.; Cheeseman, J. R.; Zakrzewski, V. G.; Montgomery, J. A., Jr.; Stratmann, R. E.; Burant, J. C.; Dapprich, S.; Millam, J. M.; Daniels, A. D.; Kudin, K. N.; Strain, M. C.; Farkas, O.; Tomasi, J.; Barone, V.; Cossi, M.; Cammi, R.; Mennucci, B.; Pomelli, C.; Adamo, C.; Clifford, S.; Ochterski, J.; Petersson, G. A.; Ayala, P. Y.; Cui, Q.; Morokuma, K.; Malick, D. K.; Rabuck, A. D.; Raghavachari, K.; Foresman, J. B.; Cioslowski, J.; Ortiz, J. V.; Baboul, A. G.; Stefanov, B. B.; Liu, G.; Liashenko, A.; Piskorz, P.; Komaromi, I.; Gomperts, R.; Martin, R. L.; Fox, D. J.; Keith, T.; Al-Laham, M. A.; Peng, C. Y.; Nanayakkara, A.; Gonzalez, C.; Challacombe, M.; Gill, P. M. W.; Johnson, B.; Chen, W.; Wong, M. W.; Andres, J. L.; Head-Gordon, M.; Replogle, E. S.; Pople, J. A. *Gaussian 98*, Revision A.7; Gaussian, Inc.: Pittsburgh, PA, 1998.
(34) Duan, X.; Linder, D. P.; Page, M.; Soto, M. R. *J. Mol. Struct. (THEOCHEM)* **1999**, *465*, 231.
(35) Politzer, P.; Lane, P.; Concha, M. C. *J. Phys. Chem. A* **1999**, *103*, 1419.
(36) Steinfeld, J. I.; Francisco, J. S.; Hase, W. L. *Chemical Kinetics and Dynamics*; Prentice Hall: Englewood Cliffs, NJ, 1999.
(37) Chase, M. W.; Davies, C. A.; Downey, J. R., Jr.; Frurip, D. J.; McDonald, R. A.; Syverud, A. N. *J. Phys. Chem. Ref. Data* **1985**, Suppl. No. 1.
(38) Wang, Z.-X.; Huang, M.-B. *J. Am. Chem. Soc.* **1998**, *120*, 6758.
(39) Gurvich, L. V.; Veyts, I. V.; Alcock, C. B. *Thermodynamic Properties of Individual Substances*, 4th ed.; Hemisphere Pub. Co.: New York, 1989.
(40) Computational Chemistry Comparison and Benchmark DataBase, NIST Standard Reference Database 101, Release 8, May 2003. http://srdata.nist.gov/cccbdb/.